JOURNAL OF MATERIALS SCIENCE **40** (2005) 1459– 1463

Texturization of multicrystalline silicon by wet chemical etching for silicon solar cells

P. PANEK, M. LIPIŃSKI, J. DUTKIEWICZ
Institute of Metallurgy and Materials Science, PAS, 25 Reymonta Str., 30-059 Cracow, Poland
E-mail: pan-kozy@wp.pl

Two kinds of surface texturization of mc-Si obtained by wet chemical etching are investigated in view of implementation in the solar cell processing. The first one was the acid texturization of saw damage on the surface of multicrystalline silicon (mc-Si). The second one was macro-porous texturization prepared by double-step chemical etching after KOH saw damage layer was previously removed.

Both methods of texturization are realized by chemical etching in HF-HNO_3-H_2O with different additives. Macro-porous texturization allows to obtain effective reflectivity (R_{eff}) in the range 9–20% from bare mc-Si. This R_{eff} value depends on the time of second step etching that causes porous structure modification. The internal quantum efficiency (IQE) of cells with this kind of texturization has possibility to reach better conversion efficiency than the standard mc-Si solar cells. However, low shunt resistance depends on morphology of porous layer and it is the main factor which can reduce open circuit voltage and conversion efficiency of cells.

The effective reflectivity is about 17% for acid texturized mc-Si wafer. The investigation of surface morphology by scanning electron microscopy (SEM) revealed that the dislocations are appearing during chemical etching and they can reduce open circuit voltage. The density of the dislocations can be reduced by controlling depth of etching and optimisation of acid solution.

1. Introduction

Nowadays, the mc-Si is the most important base material for solar cells production [1]. In the last decade considerable progress has been made in improving industrial solar cell efficiency due to application plasma enhanced chemical vapour deposition (PECVD) SiN_x [2]. The further improvement will be possible if effective texturization is involved in cells production. It is known that texturization can increase a short-circuit current due to three mechanism ways. The most important is reduction of reflectance. The next one is light trapping in the volume of the silicon wafer. The third one is higher light absorption closer to the junction in comparison with planar surface [3].

The simple method based on anisotropic alkaline etching commonly used for (100) oriented monocrystalline wafers textures surface with random pyramids. In the case of multicrystalline Si this method is not effective because there are few (100) oriented grains on mc-Si wafer, but it is generally used for saw damage removal.

Many techniques for texturing mc-Si have been investigated in the past. Some of them have been based on the use of RIE [4, 5], others on isotropic wet acidic etching [6, 7] or porous silicon formation [8].

In this work, we present the results of the optical and structural investigation of texturized surfaces, obtained by two methods based on wet chemical etching. The first method is based on HF-HNO_3 etching of as-cut mc-Si wafers in one process. The second one, more sophisticated, applied after KOH saw damage etching is based on two-step chemical acid etching.

2. Experiments

The substrates used in this work were "as-cut", *p*-type, 1 Ω cm multicrystalline (mc-Si) silicon wafers "Baysix". Experimental solar cells were fabricated on the basis of the screen-printing technique used at the IMMS PAS [9, 10]. The typical process sequence can be presented in the following steps: (1) Saw damage etching and texturization, (2) Junction n^+-*p* formation by phosphorous diffusion, (3) Phosphorous silica glass (PSG) removing, (4) Passivation by thermal oxidation, (5) ARC TiO_x spray-on deposition, (6) Screen-printing of contacts, (7) Firing in IR furnace. For one series of cells, the PSG layer was not removed and it was used as passivation layer.

The total reflectivity of the samples as a function of the wavelength was measured using Perkin–Elmer Lambda-9 spectrophotometer equipped with an integrating sphere. The effective reflectivity was calculated by integrating the reflectivity losses under AM1.5 standard solar illumination from 400 to 1100 nm.

The SEM and transmission electron microscopy (TEM) were used for surface structure investigation. Additionally the porous structures were investigated by mercury porosimetry through the use of Carlo Erba—Porosimeter 2000 and by nitrogen sorption method through the use of ASAP 2010 Micromeritics. Sheet resistance of emitters $R_s(n^+)$ was measured by four point probe. The current-voltage (I-V) characteristics and IQE were measured for electrical characterization of solar cells with different kinds of surface texturization.

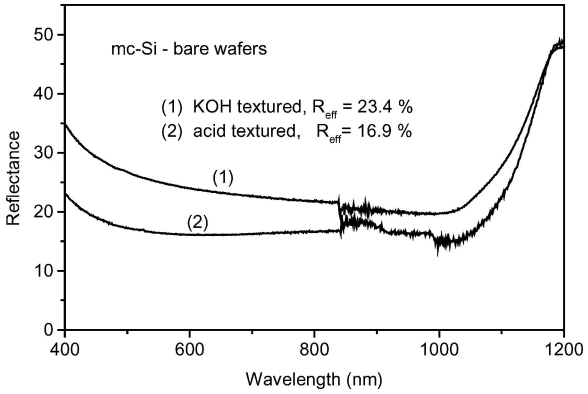

Figure 2 Reflectance of KOH etched and acid textured multicrystalline silicon wafers.

3. Results and discussion

3.1. Acid texturization

For acidic etching in 10HF:1HNO_3:1H_2O (vol.) solution the removal of saw damage layer and the surface texturing was obtained in one step. The etching rate is about 3 μm/min. Because the solutions produce simultaneously nano-porous layer which is unfavourable for solar cells manufacturing (high resistivity, high absorption and recombination) it is removed in KOH solution. Fig. 1 shows the morphology of the surface after 15 s and after 60 s of acidic etching. It can be seen that after 15 s very narrow slots are formed. After 60 s the surface is covered by oval pits whose size is in the range 5–10 μm and the structure of these pits is independent on the grains orientation.

The figures obtained by first eatching process are typical for micro-cracks of the damaged layer after slicing exposed by selective etching. The kinetics of pits formation is determined by high speed of etching along the cracks' surface due to very fast diffusion of the solution into the cracks. If the time of etching is too long, the texturization disappears and the dislocations and grains boundary figures appear. This can cause mechanical weakening of the wafers and additionally it can causes problems with shunting of the solar cells' junction. The decrease of reflectivity by acid texturing can be seen in Fig. 2.

The effective reflectivity (R_{eff}) calculated for 400–1100 nm range of wavelength AM1.5 spectral distribution was reduced from 23.4 to 16.9%.

The electrical parameters of cell with acidic texturization are presented in Table I. It shows that acid texturization allows to increase short circuit current density J_{sc} about 6% in comparison with cell having KOH texturized surface.

TABLE I Electrical parameters of solar cells

No.	Text.	J_{sc} (mA/cm^2)	r_{sh} (kΩcm^2)	r_s (Ωcm^2)	V_{oc} (mV)	FF (%)	E_{ff} (%)
1	Acidic	30.12	1.1	0.51	586	73.2	12.92
2	KOH	28.40	2.9	0.75	588	75.9	12.64

3.2. Macro-porous texturization

The mc-Si wafers were firstly etched in KOH solution to remove saw damage layer of about 10 μm from each side. Afterwards, the (macro-) porous silicon (PSi) was formed into one solution and modified into the second one. The solution for PSi formation named "C1" was following: 2HF(40%):

TABLE II Optical and morphological characteristic of the mc-Si surface with PSi layer

Porous Si stucture in Fig. 2.	Process technology —the PSi layer	R_{eff} (%)	Average size of the pores (nm)	S_{PSi} /S_{flat}
a	C1 solution (20 min)	9.3	~30	50
b	C1 + 40 s in C2	12.6	~200	29
c	C1 + 90 s in C2	17.1	~500	23
d	C1 + 300 s in C2	21.1	~800	18

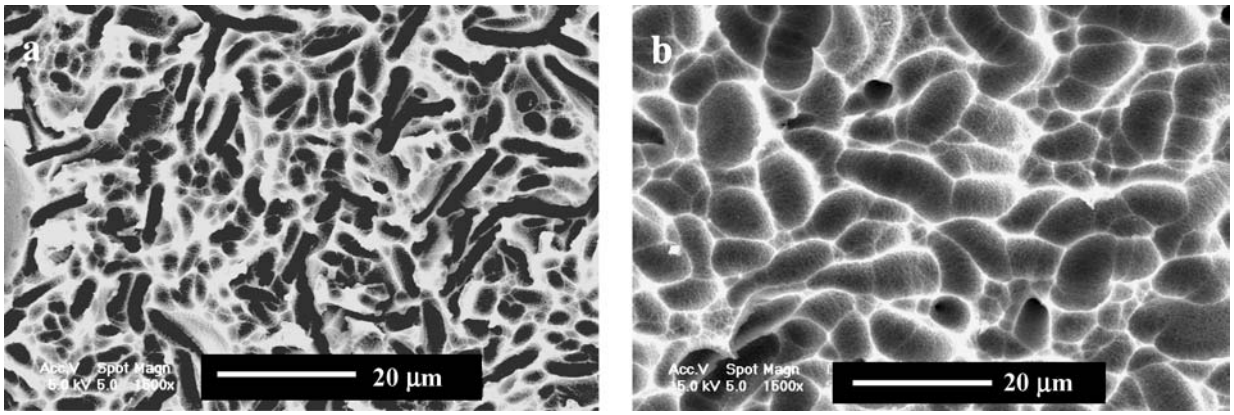

Figure 1 SEM photograph (plan view) of mc-Si surface after 15 s (a) acid etching and after 60 s (b) acid etching.

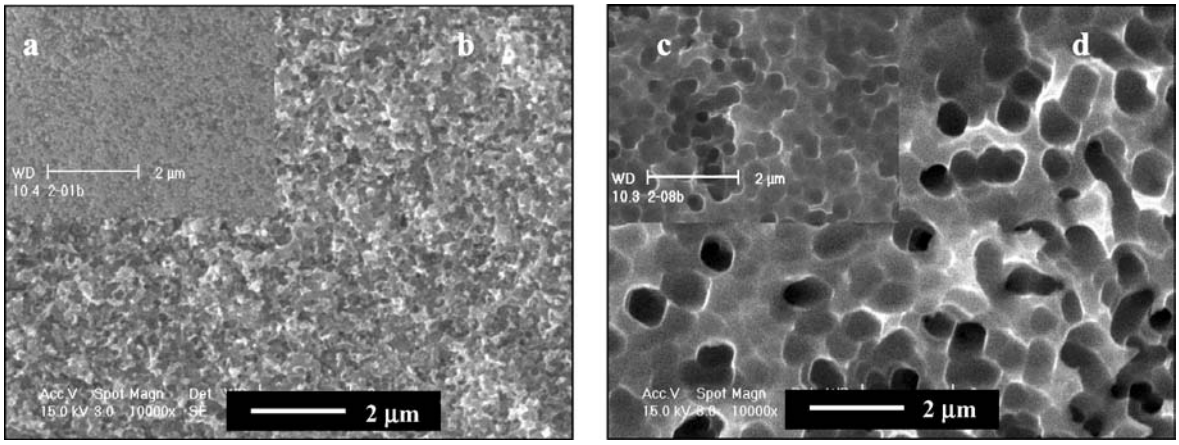

Figure 3 SEM micrographs of mc-Si with PSi layer obtained by wet acid etching in C1 solution (a) and next modified in C2 solution at 40 s (b), 90 s (c) and 300 s (d). The magnification SEM pictures is marked.

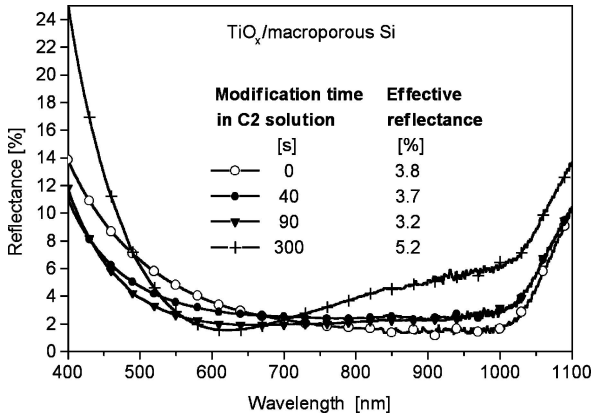

Figure 4 The reflectance of solar cells with PSi, PSG and TiO_2 layer (series B) and calculated effective reflectance coefficients. For mc-Si solar cell without any PSi layer (Series B) the effective reflectance was 9.14%.

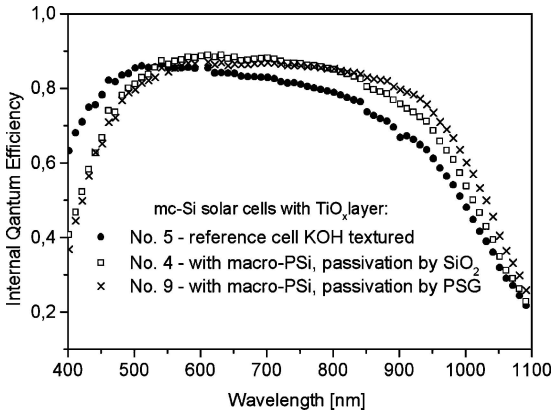

Figure 5 Internal quantum efficiency for best solar cells presented in Table III.

$1HNO_3(65\%):2H_2O:2H_2O_2:1C_2H_5OH$ (vol.). The second solution used for modification of PSi layer named "C2" was following: $2HF:98HNO_3$ (vol.). The etching time in C1 solution was 20 min and in C2 solution was in the range from 0 s to 300 s what result is the surface morphology shown in Fig. 3.

The summarized results optical and TEM analysis of the PSi layers are presented in Table II. It shows that the pores size can be controlled by etching time in C2 solution. By SEM and TEM observation of the cross-sections of the porous layer, the pore diameters are found to be comparable to their depth and the structure of the pores is independent of the grains orientation. The porous layers reported here have been homogeneous on the whole surface of 25 cm^2 of each mc-Si wafer.

3.3. Solar cells characterization

The solar cells on mc-Si wafers with PSi layers were prepared consistently with technology described in

TABLE III The main electrical parameters I-V light characterisics of mc-Si cells with PSi layer for different time of etching in "C2 solution" (t = 0, 40, 90, and 300 s) and reference cells without porous Si layer obtained during the same technology process

No.	t (s)	J_{sc} (mA/cm^2)	V_{oc} (mV)	r_{sh} (kΩcm^2)	r_s(Ωcm^2)	J_{s1} (pA/cm^2)	J_{s2} (μA/cm^2)	FF (%)	E_{ff} (%)
			Solar cells with PSi layer and thermal oxide—Series A						
1	0	27.4	544	0.31	2.0	3.8	0.56	65.8	9.81
2	40	27.4	570	0.33	1.8	3.7	0.18	72.0	11.25
3	90	27.6	569	0.96	1.6	3.7	0.19	74.7	11.75
4*	300	31.4	586	1.32	2.1	3.6	0.15	70.8	13.02
5*	Reference	28.8	573	1.78	1.8	3.7	0.18	73.4	12.15
			Solar cells with PSi layer and PSG layer—Series B						
6	0	28.6	504	0.24	2.5	3.5	1.5	61.6	8.89
7	40	28.2	582	0.13	2.3	3.4	0.16	61.7	10.32
8	90	28.5	579	0.48	1.7	3.5	0.17	73.2	12.10
9*	300	28.9	582	0.74	1.4	3.3	0.15	75.7	12.74
10	Reference	28.0	576	1.86	1.6	3.6	0.17	74.7	11.89

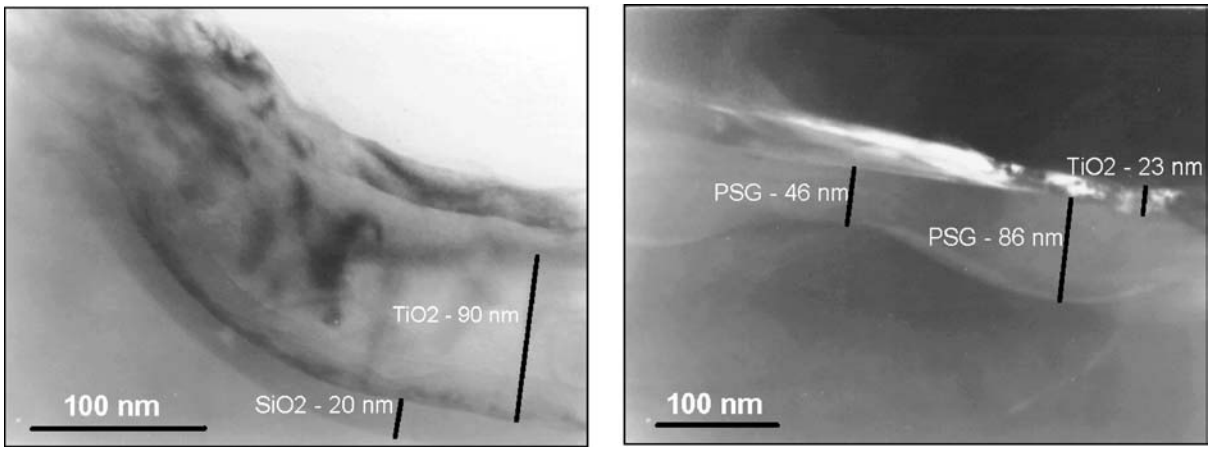

Figure 6 TEM micrographs revealing the top layers through the thickness of the front surface structure of the solar cells with PSi after etching for 300 s in C2 solution in the case of thermal oxide (a—bright field TEM image) and PSG (b—dark field TEM image).

Ref. [9]. According to new concept, the phosphorosilica glass (PSG) was left on the second series of the cells after emitter doping process from $POCl_3$ [10, 11].

The measurements of I-V characteristics of the solar cells allow to determine the basic parameters like: I_{sc}—short circuit current, V_{oc}—open circuit voltage, FF—fill factor and E_{ff}—efficiency. The I-V curves were numerically fitted with the double diode exponential relationship of the following form:

$$I = I_{ph} - I_{s1}\left[\exp\left(\frac{V + I \cdot R_s}{A_1 V_t}\right) - 1\right] - I_{s2}\left[\exp\left(\frac{V + I \cdot R_s}{A_2 \cdot V_t}\right) - 1\right] - \frac{V + I \cdot R_s}{R_{sh}} \quad (1)$$

where I_{ph}—generated photocurrent, R_s—series resistance, R_{sh}—shunt resistance, $A_1 = 1$ and $A_2 = 2$ diode ideality factors, I_{s1} and I_{s2} saturation currents, V_t is equal to kT/e where k, e and T have their usual meaning.

Table III contains the main electrical parameters of solar cells which area was 25 cm^2 with macro-PSi layer and they are compared with parameters of reference cells with surfaces texturized in KOH. The r_s and r_{sh} means the specific value of series and shunt resistance defined by $r_s = R_s \times$ area, $r_{sh} = R_{sh} \times$ area respectively.

The reflectance of solar cells of series B and calculated effective reflectance coefficients are presented in Fig. 4.

The effective reflectance coefficient for mc-Si with PSi modified layers in C2 solution was reduced to more than 5.2% for solar cells with double ARC layer (PSG + TiO_2). The internal quantum efficiency (IQE) for the best cells with PSi and reference cell are presented in Fig. 5.

In the full wavelength range the IQE of the solar cells with PSi layer (without modification in C2 solution) is low. After 300 s of modification, IQE is higher in the 600–1100 nm wavelength range than for conventional mc-Si cell which can be caused by increased light—trapping. Unfortunately, the surface passivation did not improve the IQE for mc-Si with PSi layer for short wavelengths.

The TEM studies allow to observe layers on the front side of the solar cells. Using the diffraction pattern related to particular layer they were defined and additionally the thickness of the layers was determined. For example the TiO_2 at 300°C using $(C_2H_5OH)_4Ti$ as precursor was deposited by spray method and after fired in IR furnace at 880°C it has a form of anataz.

The PSG layer on PSi (Fig. 6b) has not homogeneous thickness. The TiO_2/SiO_2 and TiO_2/PSG antireflection coatings do not fulfill the optimal ARC conditions but their combination with PSi layer give effective reflectance below 5%.

The PSi texture causes an inhomogeneous depth of the junction after diffusion and big phosphorous concentration in the peaks and walls between pores. Some part of the light is absorbed in the top region of the peaks and walls where take place big recombination of curriers. This can be seen in Fig. 5 for the IQE short wavelength regime. The same problem for reactive ion etching was observed by Dekkers *et al*. [12]. The solar cells with PSi layer obtained only in C1 solution has worse open circuit voltage V_{oc} which is caused mainly by higher values of I_{s2} saturation currents and shunt resistance r_{sh} (see Table III). The modification treatment reduce the development of a surface what improves I_{s2} and r_{sh} which for solar cell modified 300 s reach the values of parameters for reference cells. Additionally, the increase of the short-circuit current and fill factor of cells after modification treatment in C2 solution improves the V_{oc} value.

4. Conclusions

The structures of the texturized surfaces reported here are independent of the crystallographic orientation of the mc- Si grains. The acid texturization can reduce the average effective reflectance to about 17%, which is lower than in the case of alkaline texturization. It is shown that acid texturization allows to increase J_{sc} to about 6% in comparison with cell having KOH texturized surface. The higher increase of J_{sc} about 9% was obtained for the double-step chemical texturization.

Moreover, the efficiency of cells with two kinds of texturization were comparable because the cells with macro-PSi texturization have lower fill factor values.

It has been shown that the double-step chemical etching of 1 Ω·cm resistivity, *p*-type mc-Si in HF-HNO_3 based solutions can be used to form pores with diameter from about 30 nm to about 800 nm which form surface texture. For the mc-Si solar cells with PSi modified for 300 s the E_{ff} is on the level of 13% which is better in comparison with cell having KOH texturized surface.

Acknowledgements

This work was funded by the Polish State Committee for Scientific Research—contract No. 4/T08A/04623.

References

1. P. MAYCOCK, *Renewable Energy World* **7** (2003) 84.
2. B. SOPORI, *J. Electron. Mater.* **32** (2003) 1034.
3. J. A. RAND and P. A. BASORE, in Proceedings of the 22nd IEEE Photovoltaic Specialists Conference, Las Vegas, Nov. 1991, p. 192.
4. S. WINDERBAUM, O. REIHOLD and F. YUN, *Sol. Ener. Mat. Sol. Cells* **46** (1977) 239.
5. D. RUBY, S. ZAIDI, M. ROY and M. NARAYANAN, in Proceedings of the 28th IEEE Photovoltaic Specialists Conference, Anchorage, September 2000, p. 75.
6. S. DE WOLF, P. CHOULAT, E, VAZSONYJ, R. EINHAUS, E. VAN KERSCHAVER, K. DE CLERQ and J. SZLUFCIK, in Proceedings of the 16th European Photovoltaicas Solar Energy Conference, Glasgow, May 2000, edited by H. Scheer, B. McNelis, W. Palz, H.A. Ossenbrink, and P. Helm (James & James, London, 2000) p. 1521.
7. J. SZLUFCIK, F. DUERINKX, J. HORZEL, E. VAN KERSCHAVER, H. DEKKERS, S. DE WOLF, P. CHOULAT, C. ALLEBE and J. NIJS, *Sol. Ener. Mat. Sol. Cells* **74** (2002) 155.
8. R. LÜDEMANN, B. M. DAMIANI and A. ROHATGI, in Proceedings of the 28th IEEE Photovoltaic Specialists Conference, Anchorage, Sept. 2000, p. 299.
9. P. PANEK, M. LIPIŃSKI, E. BELTOWSKA-LEHMAN, K. DRABCZYK and R. CIACH, *Opto-Electr. Rev.* **11** (2003) 269.
10. K. DRABCZYK, P. PANEK and M. LIPIŃSKI, *Sol. Ener. Mat. Sol. Cells* **76** (2003) 545.
11. B. C. CHAKRAVARTY, P. N. VINOD, S. N. SINGH and B. R. CHAKRABORTY, *Sol. Ener. Mat. Sol. Cells* **73** (2002) 59.
12. H. F. W. DEKKERS, F. DUERINCKX, J. SZLUFCIK and J. NIJS, *Opto-Electr.Rev.* **8** (2000) 311.